

Chen ZHANG, Guoliang AN, Liwei WANG, Shaofei WU

# Multi-stage ammonia production for sorption selective catalytic reduction of $\text{NO}_x$

© Higher Education Press 2021

**Abstract** Sorption selective catalytic reduction of nitrogen oxides ( $\text{NO}_x$ ) (sorption-SCR) has ever been proposed for replacing commercial urea selective catalytic reduction of  $\text{NO}_x$  (urea-SCR), while only the single-stage sorption cycle is hitherto adopted for sorption-SCR. Herein, various multi-stage ammonia production cycles is built to solve the problem of relative high starting temperature with ammonia transfer (AT) unit and help detect the remaining ammonia in ammonia storage and delivery system (ASDS) with ammonia warning (AW) unit. Except for the single-stage ammonia production cycle with  $\text{MnCl}_2$ , other sorption-SCR strategies all present overwhelming advantages over urea-SCR considering the much higher  $\text{NO}_x$  conversion driven by the heat source lower than  $100^\circ\text{C}$  and better matching characteristics with low-temperature catalysts. Furthermore, the required mass of sorbent for each type of sorption-SCR is less than half of the mass of AdBlue for urea-SCR. Therefore, the multifunctional multi-stage sorption-SCR can realize compact and renewable ammonia storage and delivery with low thermal energy consumption and high  $\text{NO}_x$  conversion, which brings a bright potential for efficient commercial de- $\text{NO}_x$  technology.

**Keywords** selective catalytic reduction (SCR), nitrogen oxides ( $\text{NO}_x$ ), ammonia, composite sorbent, chemisorption

## 1 Introduction

Nitrogen oxides ( $\text{NO}_x$ , including  $\text{N}_2\text{O}$ ,  $\text{NO}$ ,  $\text{NO}_2$ ,  $\text{N}_2\text{O}_3$ ,  $\text{N}_2\text{O}_4$ , and  $\text{N}_2\text{O}_5$ ) primarily emitted from factories, power stations and automobiles are regarded as the main cause of

acid rain, photochemical smog, greenhouse effects, and  $\text{PM}_{2.5}$  [1,2]. It has been reported that with increasing oxygen concentration or increasing temperature the emissions of  $\text{NO}_x$  increase, while higher  $\text{SO}_2$  levels decrease the emissions of  $\text{NO}_x$  but increase the proportion of CO [3]. To tackle the emission of  $\text{NO}_x$  from gasoline and diesel engines, governments worldwide enact increasingly stringent policies and legislations. However, there is a growing disparity between real-world emissions and tightened standards, such as Euro VI for European Union (EU), Low Emission Vehicle (LEV) III for the USA, and CN VI for China [4,5]. The ever-increasing demand for air purification has created strong momentum for addressing  $\text{NO}_x$  emissions originated from automobiles.

As a large-scale applied  $\text{NO}_x$  reduction technology, selective catalytic reduction of  $\text{NO}_x$  (SCR) technologies reduce  $\text{NO}_x$  with reductants like  $\text{H}_2$  [6], hydrocarbon (HC) [7], and  $\text{NH}_3$  [8].  $\text{NO}_x$  can be reduced without any  $\text{CO}_2$  formation at the temperature lower than  $200^\circ\text{C}$  with  $\text{H}_2$  as the reducing agent, while  $\text{H}_2$  has been plagued by the difficulty of synthesis and storage. Hydrocarbon selective catalytic reduction of  $\text{NO}_x$  (HC-SCR) offers the potential to negate external reductant via utilizing un-burnt HC in engine exhaust stream. However, neither has been promoted to practical applications [9]. Aqueous urea solution consisting of 32.5% of urea as the ammonia precursor for the de- $\text{NO}_x$  reaction, called AdBlue in EU and diesel exhaust fluid (DEF) in the USA, can be decomposed into  $\text{NH}_3$  for reacting with  $\text{NO}_x$  in a catalytic converter (CC) to convert it into  $\text{N}_2$  and  $\text{H}_2\text{O}$ . Urea selective catalytic reduction of  $\text{NO}_x$  (urea-SCR) systems have been commercially applied in diesel vehicles since three-way catalysts are suitable for  $\text{NO}_x$  reduction in diesel and lean burning gasoline engines [10–12]. Furthermore, the nanoparticles addition applied in the fuel of internal combustion engine has a positive effect in the commercial urea-SCR technologies [13]. However, problems of low  $\text{NO}_x$  conversion efficiency and poor activity at a low temperature [14], coking caused by incomplete decomposition [15], urea crystallization [16,17], and low

Received Jul. 6, 2021; accepted Oct. 21, 2021; online Jan. 1, 2022

Chen ZHANG, Guoliang AN, Liwei WANG (✉), Shaofei WU  
Institute of Refrigeration and Cryogenics, Key Laboratory of Power Machinery and Engineering of the Ministry of Education, Shanghai Jiao Tong University, Shanghai 200240, China  
E-mail: lwwang@sjtu.edu.cn

effective ammonia content [18] require further development of better ammonia precursors to replace urea solution.

Alternative reducers should be decomposed into ammonia without producing harmful products and be easy to store and transport at an affordable cost and a wide availability from a technical and commercial standpoint. The ammonia precursors studied can be classified into active carbon (AC), Zeolite, ammonium carbamate, ammonium formate, methanamide and guanidinium formate, ammonium salt, and ammoniate. The ammonia capture capacities of AC and Y-zeolite with on-site ammonia synthesis are increased compared with non-treated AC and Y-zeolite due to ammonium ion formation and ammine complex formation, respectively [19]. However, their ammonia capture capacities are still too low compared with those of ammoniates. The guanidinium salts with higher decomposition temperatures present larger ammonia densities than ammonium carbamate and urea [20]. The formamide-based mixtures are less efficient compared with urea-based agents but their NH<sub>3</sub> slip processes are better prevented [21], while ammonium salts and ammoniates offer better ammonia storage performance than solid urea [22]. The on-board ammonia storage and delivery system (ASDS) with the ammoniate-based SCR technology has the advantages of high density and direct ejecting of ammonia for de-NO<sub>x</sub> [23]. For instance, after being compressed to 1219 kg/m<sup>3</sup>, [Mg(NH<sub>3</sub>)<sub>6</sub>]Cl<sub>2</sub> occupies a volume and weight 3.1 and 2.8 times less than those of AdBlue, respectively [24]. The thermodynamic stability of the monoamine phase ([Sr(NH<sub>3</sub>)]Cl<sub>2</sub>), the diamine phase ([Sr(NH<sub>3</sub>)<sub>2</sub>]Cl<sub>2</sub>), and the octopamine phase ([Sr(NH<sub>3</sub>)<sub>8</sub>]Cl<sub>2</sub>) has also been verified to explain the working principle of strontium chloride as the ammonia sorbent for sorption selective catalytic reduction of NO<sub>x</sub> (sorption-SCR) [25]. To improve the heat and mass transfer performance and avoid agglomeration of ammoniates, expanded natural graphite treated with sulfuric acid (ENG-TSA) is added as the matrix for ammoniates (CaCl<sub>2</sub>, SrCl<sub>2</sub>, BaCl<sub>2</sub>, NH<sub>4</sub>Cl, and NaBr) to complete sorption-SCR [26,27], with an annual required mass/volume and cost generally lower than those of urea-SCR. Furthermore, due to the advantage of the relatively lower starting temperature for desorbing ammonia compared with AdBlue (over 160°C), the NO<sub>x</sub> conversion of sorption-SCR with CaCl<sub>2</sub>/ENG-TSA is around 45% higher than that of the urea-SCR at 50°C [28]. Therefore, it can be concluded that ammoniates with the matrix of ENG-TSA bring a bright future for safe and efficient NH<sub>3</sub> selective catalytic reduction of NO<sub>x</sub> (NH<sub>3</sub>-SCR).

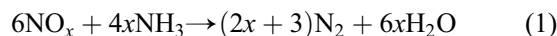
However, only the single-stage sorption cycle is hitherto adopted for sorption-SCR. The existing single-stage sorption-SCR problems lie in balancing the pressure stability and the proper starting temperature as well as in quick launching and detecting the remaining ammonia in the ASDS. Multi-stage sorption cycles based on ammonia

sorption and resorption principles have been utilized and verified in thermal energy conversion applications, such as refrigeration [29], heat transformer [30], and thermal energy storage [31]. To realize compact and renewable ammonia storage and delivery with a low thermal energy consumption and a high NO<sub>x</sub> conversion, the multi-functional multi-stage ammonia production cycles are first proposed and studied under the working condition of sorption-SCR. After that, the proper ammoniate-ammonia working pairs are selected and tested to obtain their thermodynamic performance. Based on thermodynamic models, the starting temperature, NO<sub>x</sub> conversion, ammonia storage density, thermal efficiency of ammonia production, and bulk weight and volume of single and multi-stage ammonia production cycles are compared with AdBlue as the benchmark material.

## 2 Working principle

### 2.1 Mechanism of sorption-SCR

Essential reactions for five NO<sub>x</sub> formation pathways (the thermal formation pathway, the prompt formation pathway, the N<sub>2</sub>O formation pathway, the NO<sub>2</sub> formation pathway, and the NNH formation pathway) have ever been summarized [32], while the chemistry of the NO<sub>x</sub> destruction via NH<sub>3</sub>-SCR can be expressed in Eq. (1), which occurs in a SCR catalytic converter (SCR-CC).



As shown in Fig. 1(a), the typical sorption-SCR system consists of an ASDS (including ammoniates, electric heaters, inner exhaust pipes, and ammonia charging pipes), a nozzle, an SCR-CC (including carrier, catalyst and encapsulation), an SCR electronic control unit (SCR-ECU), several valves for controlling exhaust flow and ammonia flow, as well as sensors for temperature, pressure, NO<sub>x</sub> and NH<sub>3</sub> detection.

For the on-board de-NO<sub>x</sub> phase, the ASDS is pre-heated by the electric heater, while the heating source could be switched to the exhaust gas for saving electricity after the vehicle is started. As soon as the pressure of the ASDS reaches around 0.4–0.5 MPa, the valve between the ASDS and the nozzle is opened for ejecting NH<sub>3</sub> via the nozzle and mixing it with the exhaust gas. After the mixture is catalyzed in the SCR-CC (Eq. (1)), the products will go through the NH<sub>3</sub> sensor and NO<sub>x</sub> sensor, which return the feedback signal to the SCR-ECU for adjusting the amount of NH<sub>3</sub> ejection via the temperature control and the electromagnetic valve control.

If the NH<sub>3</sub> stored in the ASDS is almost used up, the NH<sub>3</sub> capture and storage phase (Fig. 1(b)) will proceed when connecting the ASDS with an external ammonia tank. When the pressure of the ASDS is lower than that of

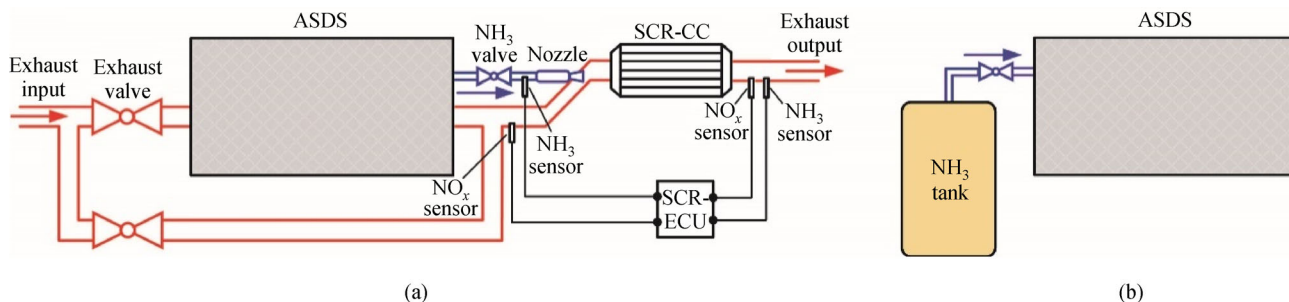


**Fig. 1** Working principle of sorption-SCR. (a) On-board de-NO<sub>x</sub>-phase; (b) off-board ammonia capture and storage phase.

the ammonia tank, the valve between the ASDS and the ammonia tank is opened for ammonia capture and storage in the ASDS until researching sorption saturation, with the sorption temperature of the ASDS controlled by the external cooling method. The specific working principle of the ASDS can be presented by the Clapeyron diagram.

2.2 Single-stage ammonia production

The single-stage ammonia production process is shown in Fig. 2, i.e., the ammonia capture and storage phase and the de-NO<sub>x</sub> phase, whose process are detailed as follows:

1) When the ammonia stored in the ASDS is not efficient, the ammonia capture and storage phase proceeds. The temperature of the ammonia tank ( $T_a$ ) is controlled and its state keeps at point 1 in the NH<sub>3</sub> line, while the initial state of the ammoniate inside the ASDS is at point 3 in the ammoniate line. After opening the valve between the ammonia tank and the ASDS, the ammoniate state will change into point 2 since its pressure is limited by the pressure of ammonia tank ( $p_a$ ) while its temperature increases because of the release of the sorption heat. After achieving sorption saturation, the valve is closed, and the ammoniate could be cooled back to point 3.

2) During vehicle driving, only the de-NO<sub>x</sub> phase is required. The ASDS is heated from point 3 to point 4 and

then the valve between the ASDS and the nozzle is opened for ejecting ammonia at point 5. It needs to be mentioned that point 5 locates at the right of ammoniate line as the actual desorption pressure has to be lower than the threshold desorption pressure.

The starting temperature is too high for high-temperature ammoniate, while the pressure vibration is so violent that it is difficult to be controlled within the safety pressure for low-temperature ammoniate. Therefore, the ammonia storage material for commercial utilization is chosen for middle-temperature ammoniate.

2.3 Double-stage ammonia production

Double-stage ammonia production is proposed to solve the problem of high starting temperature, with the specific principle shown in Fig. 3, i.e., the ammonia capture and storage phase, the ammonia transfer (AT) phase, and the de-NO<sub>x</sub> phase, whose process are described as follows:

1) The ammonia capture and storage phase of the first stage ammoniate inside the ASDS is the same as that of the single-stage ammonia production process, including points 1, 2, and 3.

2) The initial state of the second stage ammoniate inside AT unit is at point 6 with the temperature set as the ambient temperature. The ASDS is heated from points 3 to 4 and

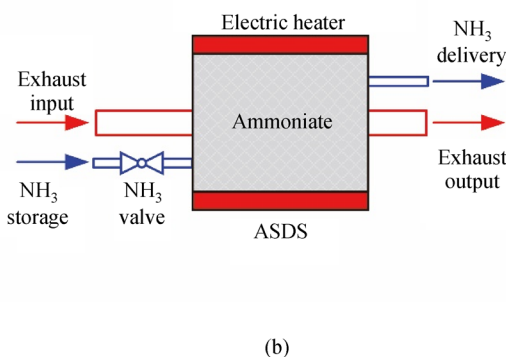
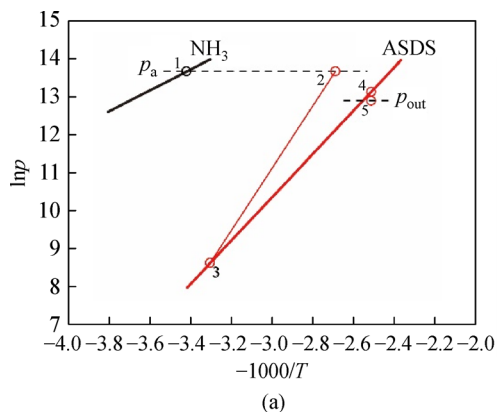


**Fig. 2** Single-stage ammonia production process. (a) Clapeyron diagram; (b) working principle.

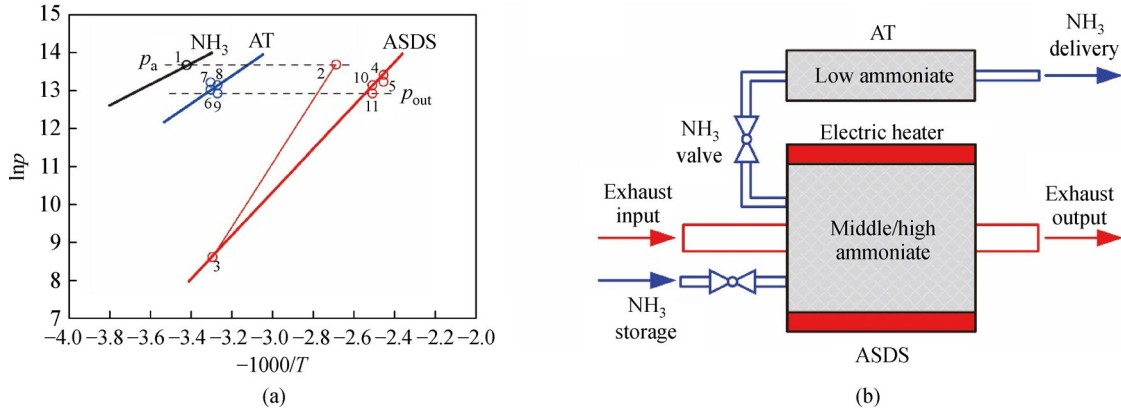


**Fig. 3** Double-stage ammonia production process. (a) Clapeyron diagram; (b) working principle.

then the valve between the ASDS and the AT unit is opened for ammonia resorption at points 5 and 7 with the same pressure. The temperatures of the ASDS and the AT unit are assumed not to change during the resorption process. After the second stage, the ammoniate achieves the sorption saturation, the valve is closed, and the first and second stage ammoniate will return to points 3 and 6, respectively.

3) The AT unit remains at point 8 and the ASDS is heated from point 3. During the initial stage of vehicle driving, the valve between the AT unit and the nozzle is opened to eject ammonia at point 9. After the ASDS is heated up to point 10, the valve between the ASDS and the AT unit is also opened for ejecting ammonia to the nozzle at point 11.

Since the ammonia desorbed from the ASDS will pass the AT unit during the de-NO<sub>x</sub> phase, the ammonia filled in the AT unit can remain in saturation, which means the AT phase is only required for the first time.

#### 2.4 Triple-stage ammonia production

Triple-stage ammonia production is progressed to help

detect the remaining ammonia in the ASDS for multi-functional consideration. The specific principle is depicted in Fig. 4, i.e., the ammonia capture and storage phase, the double step AT phase, the de-NO<sub>x</sub> phase, and the ammonia warning (AW) phase, whose process are described as follows:

1) The ammonia capture and storage phase of the first stage ammoniate inside the ASDS is the same as that of the double-stage ammonia production process, including points 1, 2, and 3.

2) The initial temperatures of the ASDS and the AW unit remain at the ambient temperature. After the valve between the ASDS and the AW unit is opened, the resorption process will occur, with the state of both the first stage ammoniate in the ASDS and the third stage ammoniate in the AW changing to point 4. If the third stage ammoniate achieves sorption saturation, the valve is closed and the first and third stage ammoniate will return to points 3 and 5, respectively. The AT process between the ASDS and the AT unit is the same as that of the double-stage ammonia production, including points 3, 6, 7, 8, and 9.

3) The de-NO<sub>x</sub> phase is also the same as that of the double-stage ammonia production, including points 10, 11,

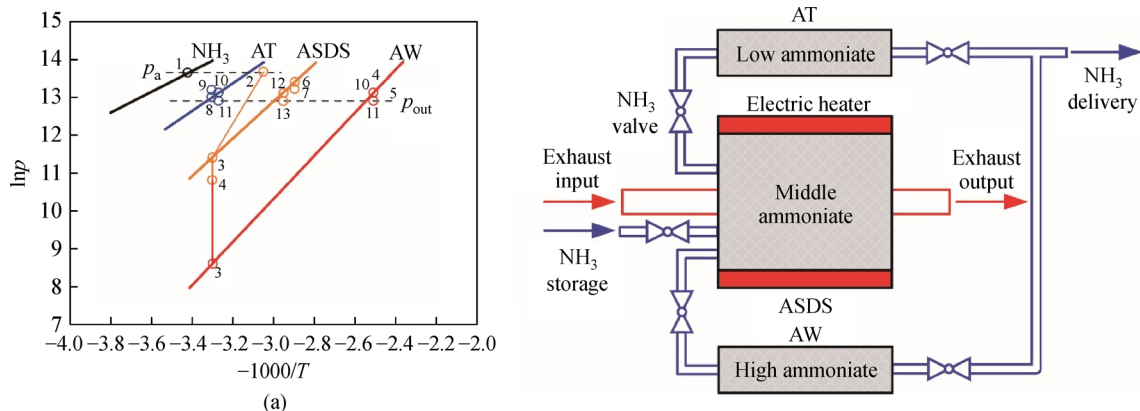


**Fig. 4** Triple-stage ammonia production process. (a) Clapeyron diagram; (b) working principle.

12, and 13.

4) If the detection results of the ammonia sensor before the nozzle present insufficient amount of ammonia output, the AW unit should be heated to point 14. After closing the valve between the AT unit and the nozzle while opening the valve between the AW unit and the nozzle, the ammonia could be ejected to the nozzle at point 15. Since ammonia is inadequate for the ASDS, the ammonia capture and storage phase as well as the AT between the ASDS and the AW unit should proceed before the next driving.

### 2.5 Double-stage triple-effect ammonia production

To pursue a more compact system, double-stage triple-effect ammonia production is designed with the same function of triple-stage ammonia production, and the specific principle is displayed in Fig. 5, i.e., the ammonia capture and storage phase, the AT phase, the de-NO<sub>x</sub> phase, and the AW phase, whose process are described as follows:

1) Multi-ammoniate is utilized in the ASDS, thus the initial states of middle-temperature ammoniate and high-temperature ammoniate are at points 3 and 4, respectively. After opening the valve between the ammonia tank and the ASDS, the states of two kinds of ammoniates will change to the same point 2. If sorption saturation is achieved, the valve will be closed and the middle- and high-temperature ammoniate will return to points 3 and 4.

2) The overall AT phase between the ASDS and the AT unit is similar to that of the double-stage ammonia production, including points 3, 4, 5, 6, 7, 8, and 9. Since the pressure of point 7 is lower than that of point 8, only the middle-temperature ammoniate can transfer ammonia to the AT unit.

3) The de-NO<sub>x</sub> phase is also the same as that of the double-stage ammonia production, including points 10, 11, 12, 13, and 14. During this phase, the high-temperature ammoniate does not react because of its much lower partial pressure at point 14.

4) When the ammonia sensor before the nozzle shows

that the amount of ammonia output is not sufficient, the ASDS should be heated to point 15 for high-temperature ammoniate ejecting ammonia to the nozzle at point 16. Before the next driving, the ammonia capture and storage phase should proceed again.

## 3 Performance assessment

### 3.1 Materials selection

The complex reaction of ammoniate-ammonia working pairs can be expressed in Eq. (2).



where  $M$  represents metal elements,  $X$  represents Cl/Br/I, and  $a$ ,  $b$ ,  $n$ , and  $m$  are the reaction constants. The starting temperature of ammoniate can be calculated based on the Clapeyron equation

$$T_{\text{sta}} = \frac{\Delta H}{\Delta S - R \cdot \ln p_{\text{sta}}}, \quad (3)$$

where  $R$  is the gas constant,  $\Delta H$  and  $\Delta S$  are the reaction enthalpy and entropy change of ammoniate, respectively. Considering the pressure difference, the starting pressure ( $p_{\text{sta}}$ ) is set as 0.5 MPa when the output pressure before nozzle ( $p_{\text{out}}$ ) is 0.4 MPa. Therefore, the ammoniates with a starting temperature lower than 150°C include PbCl<sub>2</sub> (26.6°C), NH<sub>4</sub>Cl (29°C), NaBr (32.8°C), BaCl<sub>2</sub> (37.1°C), LiCl (45.7°C), CaCl<sub>2</sub> (65.4°C), NaI (67.7°C), SrCl<sub>2</sub> (73.1°C), BaBr<sub>2</sub> (73.6°C), SrBr<sub>2</sub> (106.4°C), MnCl<sub>2</sub> (125.6°C), and CaBr<sub>2</sub> (130.5°C). Utilizing ammonia storage capacity as criterion, NH<sub>4</sub>Cl/NaBr, CaCl<sub>2</sub>/SrCl<sub>2</sub>, and MnCl<sub>2</sub> are chosen as the candidate for low, middle, and high temperature ammoniates, respectively.

However, pure ammoniates suffer from swelling and agglomeration during the sorption phase, which causes the severe attenuation of cycle ammonia storage capacity [33]. Therefore, even though the theoretical ammonia storage

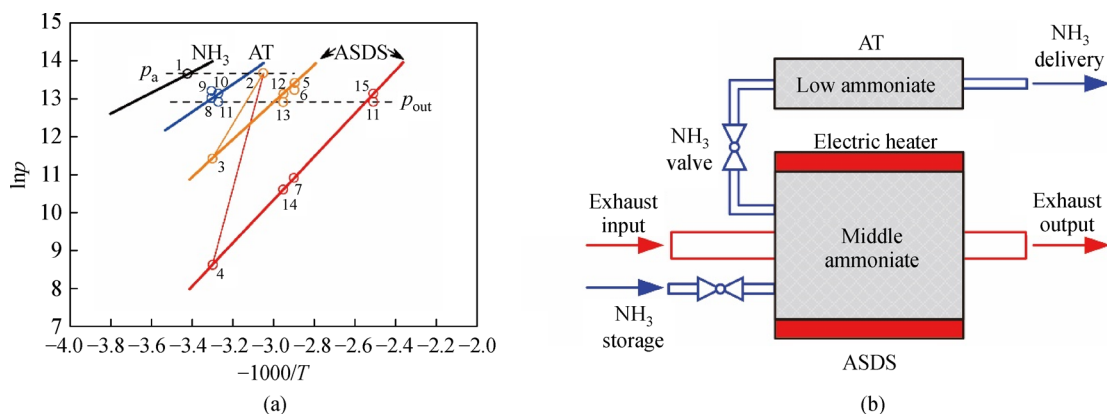


**Fig. 5** Double-stage triple-effect ammonia production process. (a) Clapeyron diagram; (b) working principle.

capacities of pure ammoniates are larger than their related composites, pure ammoniates are not recommended to be utilized in the actual system. It has been proved that ammoniates coupled with the ENG-TSA could prevent swelling and agglomeration and significantly enhance the heat and mass transfer performance over 100 times compared with pure ammoniates [34]. Thus, in this research, ENG-TSA was also applied as the ammoniates matrix to ensure its application feasibility.

### 3.2 Thermodynamic test

The thermodynamic measurement was conducted to study the relation between sorption capacity and sorbent temperature under equilibrium conditions at a constant pressure. The thermodynamic properties of composites (with NH<sub>4</sub>Cl/ENG-TSA, CaCl<sub>2</sub>/ENG-TSA, and MnCl<sub>2</sub>/ENG-TSA as examples) were tested by the Rubotherm balance (TA Instruments, America) demonstrated in Fig. 6(a). The sample was put in a steel basket suspending in a sealed steel chamber, whose temperature was controlled through thermal radiation via the circulation oil whose temperature was controlled by the thermostatic bath (SE-6, JULABO, Germany) with a temperature accuracy of 0.01 K. A PT100 temperature sensor with a precision of 0.1 K was located beneath the basket to monitor the temperature of the sorbent. The measuring chamber was connected to an ammonia tank which acted as the condenser/evaporator, whose temperature was controlled by the thermostatic glycol water bath (F32-ME, JULABO, Germany) with a temperature accuracy of 0.01 K. The working pressure of the measuring chamber was under the saturated pressure of ammonia and was detected by an absolute pressure sensor (DPI-282, Druck, UK) with a precision of 0.04%. As presented in Fig. 6(b), the initial temperature was set as low as possible for the desorption process and then moved forward to the equilibrium state that followed by increasing the tempera-

ture of thermostatic oil bath ( $T_{oil}$ ) with 5°C per step, until desorption was completed. Only after both the weight and temperature data were made stable for each step, could the temperature be increased. On the contrary, the initial temperature should be set high enough for the sorption process and  $T_{oil}$  would also be decreased by 5°C per step. The pressure was controlled within 1.0 MPa and  $T_{oil}$  kept higher than 20°C.

As manifested in Fig. 7, the thermodynamic sorption results under the condition of 0.87 MPa (corresponding to 20°C saturated ammonia) show that CaCl<sub>2</sub>/ENG-TSA and MnCl<sub>2</sub>/ENG-TSA have notable hysteresis and obvious single-point sorption characteristic, while NH<sub>4</sub>Cl/ENG-TSA has negligible hysteresis and presents multi-point sorption characteristic which leads to a higher sorption capacity.

The reaction enthalpy and entropy change of composites can be calculated with threshold reaction temperature at 0.87 MPa, 0.63 MPa and 0.44 MPa, and the relationship between  $T_s$  and sorbent pressure ( $p_s$ ) can be ensured based on Eq. (3). Figure 8 indicates that the starting temperature of NH<sub>4</sub>Cl/ENG-TSA, CaCl<sub>2</sub>/ENG-TSA, and MnCl<sub>2</sub>/ENG-TSA at 0.5 MPa are 30.9°C, 61.5°C, and 126.9°C, respectively, all of which are close enough to their theoretical value (29°C, 65.4°C, and 125.6°C). Therefore, the theoretical thermodynamic properties of sorbents are chosen for further calculation and evaluation without error bars.

### 3.3 Thermodynamic models

The thermal efficiency of ammonia production ( $\eta_{NH_3}$ ) is defined as

$$\eta_{NH_3} = \frac{m_{NH_3}}{Q_{in}} = \frac{m_{NH_3}}{Q_{sen} + Q_{des}}, \quad (4)$$

where  $m_{NH_3}$  is the total mass of ammonia production,  $Q_{in}$  is the input heat including sensible heat ( $Q_{sen}$ ) and desorption

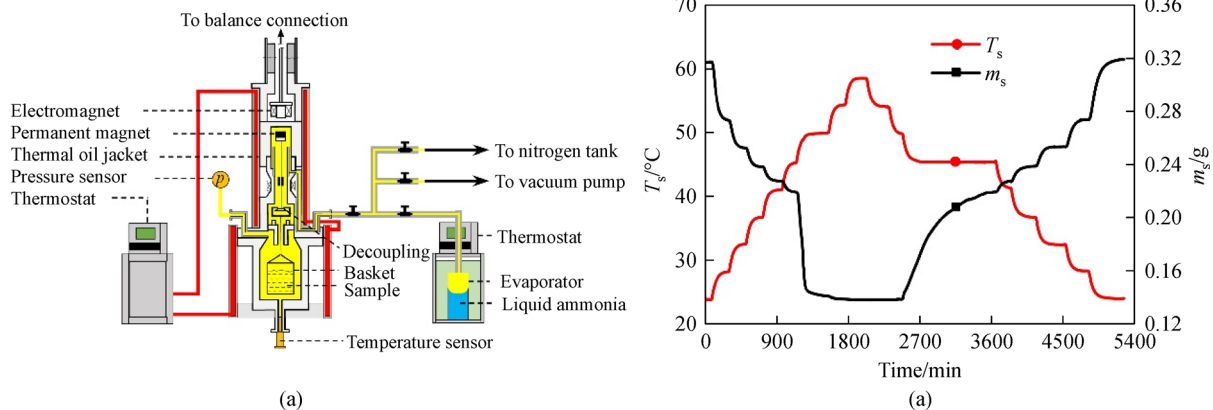
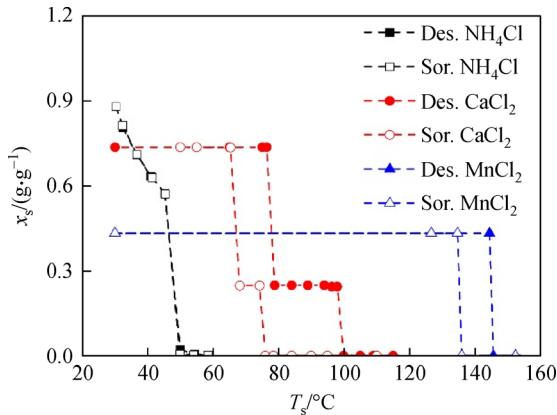
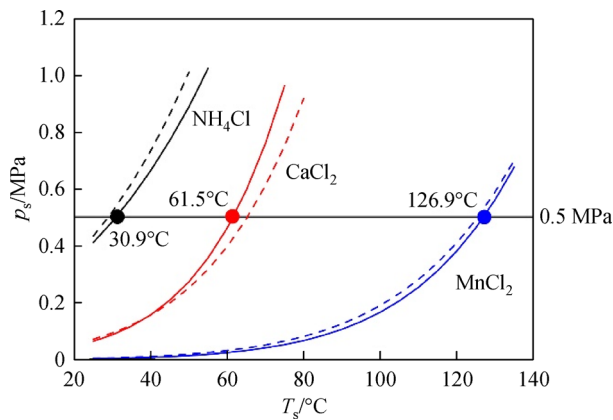


Fig. 6 Experimental test unit and test procedure.

(a) Schematic diagram of Rubotherm balance for sorption analysis; (b) test procedure of thermodynamic measurement, using NH<sub>4</sub>Cl/ENG-TSA at 0.87 MPa as an example ( $T_s$  is the sorbent temperature and  $m_s$  is the mass of the sorbent).



**Fig. 7** Thermodynamic sorption results of  $\text{NH}_4\text{Cl}/\text{ENG-TSA}$ ,  $\text{CaCl}_2/\text{ENG-TSA}$ , and  $\text{MnCl}_2/\text{ENG-TSA}$  at 0.87 MPa.



**Fig. 8**  $T_s$  versus  $p_s$  of  $\text{NH}_4\text{Cl}/\text{ENG-TSA}$ ,  $\text{CaCl}_2/\text{ENG-TSA}$ , and  $\text{MnCl}_2/\text{ENG-TSA}$ , with experimental value shown in solid lines and theoretical value shown in dash lines.

heat ( $Q_{\text{des}}$ ). The ammonia storage density ( $\rho_{\text{NH}_3}$ ) at the material level is

$$\rho_{\text{NH}_3} = \frac{m_{\text{NH}_3}}{V_s}, \quad (5)$$

where  $V_s$  is the volume of composite sorbent. For various ammonia production principles, expressions of these parameters are summarized as follows.

#### 1) Single-stage ammonia production

$$m_{\text{NH}_3} = \beta_{\text{ASDS}} \cdot x_{\text{t\_ASDS}} \cdot m_{\text{s\_ASDS}}, \quad (6)$$

where  $\beta_{\text{ASDS}}$  (0.8) is the mass proportion of ammoniate inside composite sorbent,  $x_{\text{t\_ASDS}}$  is the theoretical sorption capacity of ammoniate and  $m_{\text{s\_ASDS}}$  (1 kg) is the mass of composite sorbent for the ASDS.

$$Q_{\text{sen}} = N \cdot m_{\text{s\_ASDS}} \cdot c_{\text{s\_ASDS}} \cdot \Delta T_{\text{de\_ASDS}}, \quad (7)$$

where  $N$  is the cycle index for per kilogram composite sorbent,  $c_{\text{s\_ASDS}}$  is the specific heat of composite sorbent and  $\Delta T_{\text{de\_ASDS}}$  is the temperature increment of the ASDS

during the de- $\text{NO}_x$  phase.

$$N = \frac{m_{\text{NH}_3} \cdot D}{v \cdot t_c}, \quad (8)$$

where  $D$  (2000 km/kg) represents the valid driving distance with per kilogram ammonia,  $v$  (60 km/h) is the average driving speed, and  $t_c$  (1 h) is the average driving time for each de- $\text{NO}_x$  phase.

$$c_{\text{s\_ASDS}} = \beta_{\text{ASDS}} \cdot c_{\text{t\_ASDS}} + (1 - \beta_{\text{ASDS}}) \cdot c_{\text{ENG}}, \quad (9)$$

where  $c_{\text{t\_ASDS}}$  and  $c_{\text{ENG}}$  are the specific heat of ammoniate of the ASDS and ENG-TSA, respectively.

$$Q_{\text{des}} = m_{\text{NH}_3} \cdot \Delta H_{\text{ASDS}}, \quad (10)$$

where  $\Delta H_{\text{ASDS}}$  is the reaction enthalpy change of ammoniate of the ASDS.

$$V_s = \frac{m_{\text{s\_ASDS}}}{\rho_{\text{s\_ASDS}}}, \quad (11)$$

where  $\rho_{\text{s\_ASDS}}$  (1 g/cm<sup>3</sup>) is the density of composite sorbent of the ASDS.

#### 2) Double-stage ammonia production

$Q_{\text{des}}$  of double-stage ammonia production is the same as that of single-stage ammonia production.

$$\begin{aligned} m_{\text{NH}_3} &= \beta_{\text{ASDS}} \cdot x_{\text{t\_ASDS}} \cdot m_{\text{s\_ASDS}} \\ &= m_{\text{NH}_3\_ASDS} + m_{\text{NH}_3\_AT}, \end{aligned} \quad (12)$$

where  $m_{\text{NH}_3\_ASDS}$  and  $m_{\text{NH}_3\_AT}$  are the ammonia stored in the ASDS and the AT unit after the AT phase.

$$\begin{aligned} Q_{\text{sen}} &= m_{\text{s\_ASDS}} \cdot c_{\text{s\_ASDS}} \cdot [\Delta T_{\text{tr\_ASDS}} \\ &\quad + (N - 1) \cdot \Delta T_{\text{de\_ASDS}}], \end{aligned} \quad (13)$$

where  $\Delta T_{\text{tr\_ASDS}}$  is the temperature increment of the ASDS during the AT phase.

$$V_s = \frac{m_{\text{s\_ASDS}}}{\rho_{\text{s\_ASDS}}} + \frac{m_{\text{s\_AT}}}{\rho_{\text{s\_AT}}}, \quad (14)$$

where  $m_{\text{s\_AT}}$  and  $\rho_{\text{s\_AT}}$  (1 g/cm<sup>3</sup>) are the mass and density of composite sorbent of the AT unit, respectively.

#### 3) Triple-stage ammonia production

$$\begin{aligned} m_{\text{NH}_3} &= \beta_{\text{ASDS}} \cdot x_{\text{t\_ASDS}} \cdot m_{\text{s\_ASDS}} \\ &= m_{\text{NH}_3\_ASDS} + m_{\text{NH}_3\_AT} + m_{\text{NH}_3\_AW}, \end{aligned} \quad (15)$$

where  $m_{\text{NH}_3\_AW}$  is the ammonia stored in the AW unit after the AT phase.

$$\begin{aligned} Q_{\text{sen}} &= m_{\text{s\_ASDS}} \cdot c_{\text{s\_ASDS}} \cdot [\Delta T_{\text{tr\_ASDS}} \\ &\quad + (N - 2) \cdot \Delta T_{\text{de\_ASDS}}] \\ &\quad + m_{\text{s\_AW}} \cdot c_{\text{s\_AW}} \cdot \Delta T_{\text{de\_AW}}, \end{aligned} \quad (16)$$

where  $m_{s\_AW}$ ,  $c_{s\_AW}$ , and  $\Delta T_{de\_AW}$  are the mass, the specific heat of ammoniate, and the temperature increment during the de-NO<sub>x</sub> phase of the AW unit.

$$Q_{des} = (m_{NH_3\_ASDS} + m_{NH_3\_AT}) \cdot \Delta H_{ASDS} + m_{NH_3\_AW} \cdot \Delta H_{AW}, \quad (17)$$

where  $\Delta H_{AW}$  is the reaction enthalpy change of ammoniate of the AW unit.

$$V_s = \frac{m_{s\_ASDS}}{\rho_{s\_ASDS}} + \frac{m_{s\_AT}}{\rho_{s\_AT}} + \frac{m_{s\_AW}}{\rho_{s\_AW}}, \quad (18)$$

where  $m_{s\_AW}$  and  $\rho_{s\_AW}$  (1 g/cm<sup>3</sup>) are the mass and density of composite sorbent of the AW unit, respectively.

#### 4) Double-stage triple-effect ammonia production

$$m_{NH_3} = \beta_{ASDS} \cdot (x_{t\_ASDS\_m} \cdot m_{s\_ASDS\_m} + x_{t\_ASDS\_h} \cdot m_{s\_ASDS\_h}), \quad (19)$$

where  $x_{t\_ASDS\_m}$  and  $x_{t\_ASDS\_h}$  are the theoretical sorption capacity of middle-temperature and high-temperature ammoniate respectively, and  $m_{s\_ASDS\_m}$  and  $m_{s\_ASDS\_h}$  are the mass of composite sorbent with middle-temperature and high-temperature ammoniate for the ASDS respectively.

$$Q_{sen} = m_{s\_ASDS} \cdot \bar{c}_{s\_ASDS} \cdot [\Delta T_{tr\_ASDS} + (N-2)\Delta T_{de\_ASDS\_m} + \Delta T_{de\_ASDS\_h}], \quad (20)$$

where  $\bar{c}_{s\_ASDS}$  is the average specific heat of ammoniate of the ASDS, and  $\Delta T_{de\_ASDS\_m}$  and  $\Delta T_{de\_ASDS\_h}$  are the temperature increment of the ASDS with middle-temperature and high-temperature ammoniate during the de-NO<sub>x</sub> phase, respectively.

$$Q_{des} = m_{NH_3\_m} \cdot \Delta H_{ASDS\_m} + m_{NH_3\_h} \cdot \Delta H_{ASDS\_h}, \quad (21)$$

where  $m_{NH_3\_m}$  and  $m_{NH_3\_h}$  are the total mass of ammonia production of middle-temperature and high-temperature ammoniate respectively, and  $\Delta H_{ASDS\_m}$  and  $\Delta H_{ASDS\_h}$  are the reaction enthalpy change of ammoniate of the ASDS with middle-temperature and high-temperature ammoniate respectively.

$$V_s = \frac{m_{s\_ASDS\_m} + m_{s\_ASDS\_h}}{\rho_{s\_ASDS}} + \frac{m_{s\_AT}}{\rho_{s\_AT}}. \quad (22)$$

## 4 Results and Discussion

### 4.1 NO<sub>x</sub> conversion

Low-temperature catalysts have been studied in Refs. [35,36]. Therefore, in this section, the NO<sub>x</sub> conversion of sorption-SCR and urea-SCR is theoretically calculated

with the NO<sub>x</sub> conversion data of existing high-performance low-temperature catalyst Co-Mn-O-10 [37], as presented in Fig. 9. It is assumed that the temperatures of the CC ( $T_{cat}$ ) and the AdBlue box/ASDS ( $T_s$ ) are the same, which are both driven by co-heating of the electric heater and exhaust gas. Since the initial pyrolysis temperature of AdBlue is over 150°C [15], its practical NO<sub>x</sub> conversion remains zero within 150°C even though the theoretical NO<sub>x</sub> conversion capacity of Co-Mn-O-10 could reach almost 100%. Sorption-SCR can be divided into low starting temperature (single-stage with NH<sub>4</sub>Cl and NaBr, double-stage, triple-stage and double-stage triple-effect), middle starting temperature (single-stage with CaCl<sub>2</sub> and SrCl<sub>2</sub>), and high starting temperature (single-stage with MnCl<sub>2</sub>) driven sorption-SCR. Except for the single-stage ammonia production with MnCl<sub>2</sub>, sorption-SCR presents an overwhelming advantage over urea-SCR considering the matching characteristics with low-temperature catalysts.

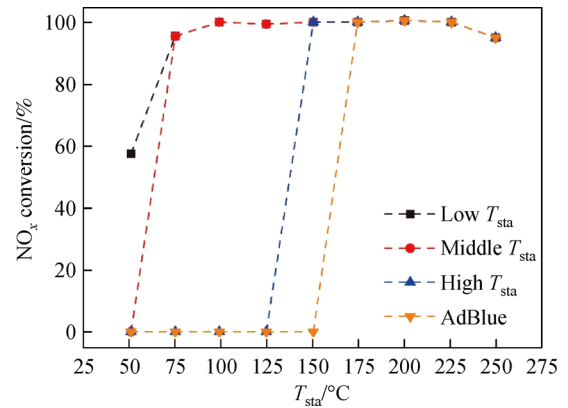
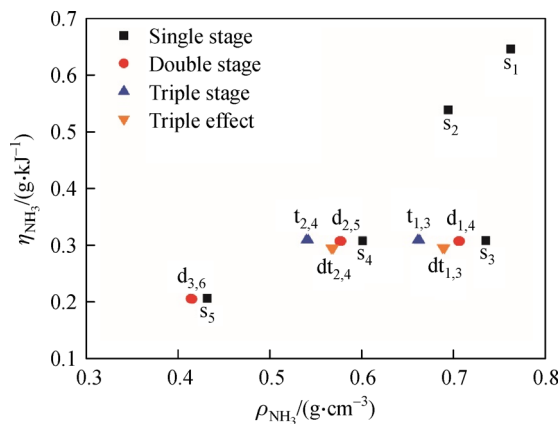


Fig. 9 Comparison of sorption-SCR and urea-SCR on NO<sub>x</sub> conversion at various driven temperatures.

### 4.2 Ammonia storage density and thermal efficiency

The  $\rho_{NH_3}$  and  $\eta_{NH_3}$  of various ammonia production processes are exhibited in Fig. 10. For single-stage ammonia production, NH<sub>4</sub>Cl (s<sub>1</sub>) has both the largest  $\rho_{NH_3}$  (0.76 g/cm<sup>3</sup>) and  $\eta_{NH_3}$  (0.65 g/kJ) with a starting temperature of 29.0°C. However, the pressure variation of NH<sub>4</sub>Cl is violent for its sole utilization. For instance, if the temperature of NH<sub>4</sub>Cl rises from 30°C to 50°C, its pressure will dramatically increase up to around 1 MPa. For double-stage, triple-stage, and double-stage triple-effect ammonia production processes, the starting temperature is decided by the ammoniate of the AT unit, i.e., 29.0°C for NH<sub>4</sub>Cl based and 32.8°C for NaBr based AT unit, while the results suggest that the type of AT unit has almost no influence on their  $\rho_{NH_3}$  and  $\eta_{NH_3}$ . Compared with SrCl<sub>2</sub>, CaCl<sub>2</sub> is more suitable as the candidate ammoniate filled in the ASDS caused by a larger  $\rho_{NH_3}$ . Therefore, the optimal ammoniate



**Fig. 10** Ammonia storage density and thermal efficiency of various ammonia production processes ( $s_1$ :  $\text{NH}_4\text{Cl}$ ;  $s_2$ :  $\text{NaBr}$ ;  $s_3$ :  $\text{CaCl}_2$ ;  $s_4$ :  $\text{SrCl}_2$ ;  $s_5$ :  $\text{MnCl}_2$ ;  $d_1$ :  $\text{CaCl}_2\text{-NH}_4\text{Cl}$ ;  $d_2$ :  $\text{SrCl}_2\text{-NH}_4\text{Cl}$ ;  $d_3$ :  $\text{MnCl}_2\text{-NH}_4\text{Cl}$ ;  $d_4$ :  $\text{CaCl}_2\text{-NaBr}$ ;  $d_5$ :  $\text{SrCl}_2\text{-NaBr}$ ;  $d_6$ :  $\text{MnCl}_2\text{-NaBr}$ ;  $t_1$ :  $\text{CaCl}_2\text{-NH}_4\text{Cl-MnCl}_2$ ;  $t_2$ :  $\text{SrCl}_2\text{-NH}_4\text{Cl-MnCl}_2$ ;  $t_3$ :  $\text{CaCl}_2\text{-NaBr-MnCl}_2$ ;  $t_4$ :  $\text{SrCl}_2\text{-NaBr-MnCl}_2$ ;  $dt_1$ :  $\text{CaCl}_2/\text{MnCl}_2\text{-NH}_4\text{Cl}$ ;  $dt_2$ :  $\text{SrCl}_2/\text{MnCl}_2\text{-NH}_4\text{Cl}$ ;  $dt_3$ :  $\text{CaCl}_2/\text{MnCl}_2\text{-NaBr}$ ;  $dt_4$ :  $\text{SrCl}_2/\text{MnCl}_2\text{-NaBr}$ ).

pairs of various principles are  $\text{CaCl}_2\text{-NH}_4\text{Cl}$  ( $d_1$ ) with  $\rho_{\text{NH}_3}$  and  $\eta_{\text{NH}_3}$  of  $0.71 \text{ g/cm}^3$  and  $0.31 \text{ g/kJ}$ ;  $\text{CaCl}_2\text{-NH}_4\text{Cl-MnCl}_2$  ( $t_1$ ) with  $\rho_{\text{NH}_3}$  and  $\eta_{\text{NH}_3}$  of  $0.66 \text{ g/cm}^3$  and  $0.31 \text{ g/kJ}$ ;  $\text{CaCl}_2/\text{MnCl}_2\text{-NH}_4\text{Cl}$  ( $dt_1$ ) with  $\rho_{\text{NH}_3}$  and  $\eta_{\text{NH}_3}$  of  $0.69 \text{ g/cm}^3$  and  $0.30 \text{ g/kJ}$ .

### 4.3 Bulk weight and volume

The bulk weight and volume of different sorption-SCR types are compared in Figs. 11 and 12 with urea-SCR as the benchmark. The least required mass of sorbents ( $m_s$ ) of different types of sorption-SCR is about 26% of  $m_{\text{AdBlue}}$  (54.5 kg) to obtain the same amount of ammonia (10.0 kg). Even for the worst candidate working pair of each type of sorption-SCR, the required  $m_s$  is less than half of  $m_{\text{AdBlue}}$ . As presented in Fig. 12, the density of compressed composite sorbents ( $\rho_s$ ) has a significant impact on the  $V_s$ , i.e., as the density increases, the volume decreases. Since 20% ENG-TSA is added as the matrix of composite sorbents,  $\rho_s$  can achieve as high as  $1.0 \text{ g/cm}^3$  with a sufficient heat and mass transfer performance for saving 60%–70% of volume. The triple-stage and double-stage triple-effect ammonia production can keep  $V_s$  smaller than that of urea-SCR ( $V_{\text{AdBlue}}$ ) with 50 L standard AdBlue, while both single-stage and double-stage with  $\text{MnCl}_2$  filled in the ASDS will occupy around 20% larger volume than  $V_{\text{AdBlue}}$  if  $\rho_s$  decreases to  $0.4 \text{ g/cm}^3$ .

### 4.4 Overall evaluation

The parameters of the single and multi-stage ammonia production cycle driven sorption-SCR are summarized in Table 1, where  $c_{\text{NO}_x}$  represents the  $\text{NO}_x$  conversion at  $75^\circ\text{C}$

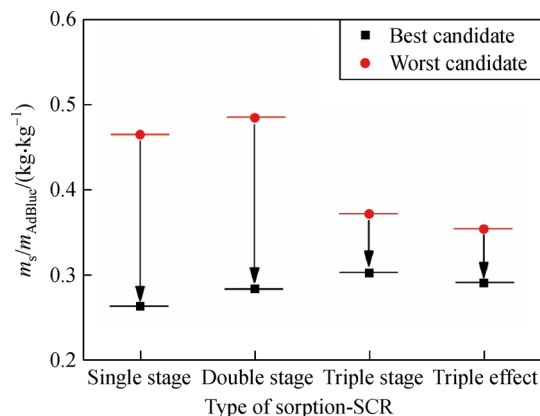


**Fig. 11** Comparison of bulk weights of different types of sorption-SCR with urea-SCR as the benchmark.

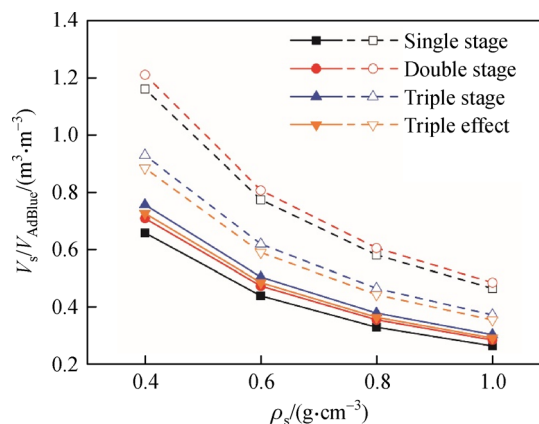


**Fig. 12** Comparison of bulk volumes of different types of sorption-SCR with urea-SCR as the benchmark (The solid lines are the best candidates and the dash lines are the worst candidate of different type of sorption-SCR).

with Co-Mn-O-10 as the catalyst, and  $V_s/V_{\text{AdBlue}}$  is the bulk volume ratio with  $\rho_s$  ranging from  $1.0$  to  $0.4 \text{ g/cm}^3$ . The symbols of de- $\text{NO}_x$  agents have coincident definitions with those in Fig. 10, where  $s_1$ ,  $d_1$ ,  $t_1$ , and  $dt_1$  represent the best candidate for the corresponding type of sorption-SCR, where  $s_5$ ,  $d_6$ ,  $t_4$ , and  $dt_4$  are the worst. It is shown that the common ground of sorption-SCR includes a lower starting temperature, higher  $\text{NO}_x$  conversion at a low temperature, a higher thermal efficiency, a larger ammonia storage capacity, and a more compact system in comparison with urea-SCR. Based on the above results, the overall evaluation of sorption-SCR types with urea-SCR as the benchmark is concluded as tabulated in Table 2. Urea-sorption only has the advantage of pressure stability over sorption-SCR. Compared with the single-stage and double-stage sorption-SCR, the triple-stage and double-stage triple-effect sorption-SCR could realize both a quick launch and an insufficient AW with the cooperation of low temperature and high temperature sorbent. Especially for

**Table 1** Parameters of types of sorption-SCRs with urea-SCR as the benchmark

De-NO <sub>x</sub> agent	$T_{\text{sta}}/^{\circ}\text{C}$	$c_{\text{NO}_x}/\%$	$\eta_{\text{NH}_3}/(\text{g}\cdot\text{kJ}^{-1})$	$\rho_{\text{NH}_3}/(\text{g}\cdot\text{cm}^{-3})$	$m_s/m_{\text{AdBlue}}$	$V_s/V_{\text{AdBlue}}$
s <sub>1</sub>	29	95.5	0.65	0.76	0.26	0.26–0.66
s <sub>5</sub>	125.6	0	0.21	0.43	0.46	0.46–1.16
d <sub>1</sub>	29	95.5	0.31	0.71	0.28	0.28–0.71
d <sub>6</sub>	32.8	95.5	0.21	0.42	0.48	0.48–1.21
t <sub>1</sub>	29	95.5	0.31	0.66	0.30	0.30–0.76
t <sub>4</sub>	32.8	95.5	0.31	0.54	0.37	0.37–0.93
dt <sub>1</sub>	29	95.5	0.30	0.69	0.29	0.29–0.73
dt <sub>4</sub>	32.8	95.5	0.30	0.57	0.35	0.35–0.88
AdBlue	160	0	0.07	0.20	1	1

**Table 2** Overall evaluation of types of sorption-SCR with urea-SCR as the benchmark

SCR type	Pressure stability	NO <sub>x</sub> conversion efficiency	Thermal efficiency	Ammonia storage capacity	Quick launch	AW
Single-stage sorption-SCR	☆☆☆	☆☆-☆☆☆	☆☆-☆☆☆	☆☆-☆☆☆	x	x
Double-stage sorption-SCR	☆☆	☆☆☆	☆☆	☆☆-☆☆☆	√	x
Triple-stage sorption-SCR	☆☆	☆☆☆	☆☆	☆☆☆	√	√
Double-stage triple-effect sorption-SCR	☆☆	☆☆☆	☆☆	☆☆☆	√	√
Urea-SCR	☆☆☆	☆	☆	☆	x	x

Note: ☆ low, ☆☆ middle, ☆☆☆ high, 'x' has no function, '√' has that function.

the double-stage triple-effect sorption-SCR, the application of multi-ammoniate as sorbent in the ASDS does not require the AW unit and thus makes the system more compact than the triple-stage sorption-SCR.

## 5 Conclusions

In this paper, various multi-stage ammonia production cycles to solve a relatively high starting temperature with the AT unit and help detect the remaining ammonia in the ASDS with the AW unit are proposed and compared with the single-stage sorption SCR and urea-SCR. The following conclusions could be reached.

Since the initial pyrolysis temperature of AdBlue is over 150°C, its practical NO<sub>x</sub> conversion remains zero within 150°C even though the theoretical NO<sub>x</sub> conversion capacity of Co-Mn-O-10 could reach almost 100%. Except for the single-stage ammonia production cycle with MnCl<sub>2</sub>, other sorption-SCR strategies have overwhelming advantages over urea-SCR considering the much higher NO<sub>x</sub> conversion driven by a heat source lower than 100°C and better matching characteristics with a low-temperature catalyst.

For single-stage ammonia production, NH<sub>4</sub>Cl has both the largest ammonia storage density ( $\rho_{\text{NH}_3}$ , 0.76 g/cm<sup>3</sup>) and thermal efficiency ( $\eta_{\text{NH}_3}$ , 0.65 g/kJ) with a starting temperature of 29.0°C. However, the pressure variation of NH<sub>4</sub>Cl is violent for its sole utilization. For double-

stage, triple-stage, and double-stage triple-effect ammonia production processes, the starting temperature is decided by the ammoniate of the AT unit, while the type of the AT unit has almost no influence on their  $\rho_{\text{NH}_3}$  and  $\eta_{\text{NH}_3}$ . Compared with SrCl<sub>2</sub>, CaCl<sub>2</sub> is more suitable as the candidate ammoniate filled in the ASDS because of the larger  $\rho_{\text{NH}_3}$ .

The least required  $m_s$  of different types of sorption-SCR is about 26% of  $m_{\text{AdBlue}}$  to obtain the same amount of ammonia. Even for the worst candidate working pair of each type of sorption-SCR, the required  $m_s$  is less than half of  $m_{\text{AdBlue}}$ . If  $\rho_s$  is controlled as 1.0 g/cm<sup>3</sup>, 60%–70% of the bulk volume of sorption-SCR ( $V_s$ ) could be saved compared with urea-SCR ( $V_{\text{AdBlue}}$ ). Even if  $\rho_s$  decreases to 0.4 g/cm<sup>3</sup>, triple-stage and double-stage triple-effect ammonia production can keep the  $V_s$  smaller than the  $V_{\text{AdBlue}}$ , while both the single-stage and double-stage with MnCl<sub>2</sub> filled in the ASDS will occupy around a 20% larger volume than  $V_{\text{AdBlue}}$ .

In summary, the advantages of sorption-SCR include a lower starting temperature, higher NO<sub>x</sub> conversion at a low temperature, a higher thermal efficiency, and a larger ammonia storage capacity in comparison with urea-SCR. In addition, by applying multi-ammoniate as sorbent, the double-stage triple-effect sorption-SCR could realize both a quick launch and an insufficient AW with a compact structure, which brings a bright potential for the efficient commercial de-NO<sub>x</sub> technology.

**Acknowledgements** This work was supported by the National Natural Science Foundation of China for the Distinguished Young Scholars (Grant No. 51825602).

SCR-CC SCR catalytic converter  
SCR-ECU SCR electronic control unit

## Notations

$c$	Specific heat capacity/( $J \cdot (kg \cdot K)^{-1}$ )
$D$	Driving distance with per kilogram ammonia/km
$m$	Mass/kg
$N$	Cycle index
$p$	Pressure/Pa
$Q$	Heat/J
$R$	Gas constant/( $J \cdot (kg \cdot K)^{-1}$ )
$t$	Time/h
$T$	Temperature/K
$v$	Average driving speed/( $km \cdot h^{-1}$ )
$V$	Volume/ $m^3$
$x$	Sorption capacity/( $g \cdot g^{-1}$ )

### Greek symbols

$\beta$	Mass proportion of ammonia inside sorbent
$\Delta H$	Enthalpy change/( $J \cdot mol^{-1}$ )
$\Delta S$	Entropy change/( $J \cdot (mol \cdot K)^{-1}$ )
$\Delta T$	Temperature difference/K
$\eta$	Thermal efficiency/( $g \cdot kJ^{-1}$ )
$\rho$	Density/( $kg \cdot m^{-3}$ )

### Subscripts

c	Cycle
de	De- $NO_x$
des	Desorption
h	High
m	Middle
out	Output
s	Sorbent
sen	Sensible
sta	Starting
t	Theoretical
tr	Transfer

### Abbreviations

ASDS	Ammonia storage and delivery system
AT	Ammonia transfer
AW	Ammonia warning
DEF	Diesel exhaust fluid
ENG-TSA	Expanded nature graphite treated by the sulfuric acid
HC	Hydrocarbon
NSR	$NO_x$ storage and reduction
SCR	Selective catalytic reduction of $NO_x$

## References

- Paolucci C, Khurana I, Parekh A A, et al. Dynamic multinuclear sites formed by mobilized copper ions in  $NO_x$  selective catalytic reduction. *Science*, 2017, 357(6354): 898–903
- Palash S M, Kalam M A, Masjuki H H, et al. Impacts of biodiesel combustion on  $NO_x$  emissions and their reduction approaches. *Renewable & Sustainable Energy Reviews*, 2013, 23: 473–490
- Miccio F, Löffler G, Wargadalam V J, et al. The influence of  $SO_2$  level and operating conditions on  $NO_x$  and  $N_2O$  emissions during fluidised bed combustion of coals. *Fuel*, 2001, 80(11): 1555–1566
- Anenberg S C, Miller J, Minjares R, et al. Impacts and mitigation of excess diesel-related  $NO_x$  emissions in 11 major vehicle markets. *Nature*, 2017, 545(7655): 467–471
- Li J, Liu H, Liu X, et al. Development of a simplified *n*-heptane/methane model for high-pressure direct-injection natural gas marine engines. *Frontiers in Energy*, 2021, 15(2): 405–420
- Väliheikki A, Petalidou K C, Kalamaras C M, et al. Selective catalytic reduction of  $NO_x$  by hydrogen ( $H_2$ -SCR) on  $WO_x$ -promoted  $Ce_{1-x}Zr_xO_2$  solids. *Applied Catalysis B: Environmental*, 2014, 156–157: 72–83
- Stere C E, Adress W, Burch R, et al. Ambient temperature hydrocarbon selective catalytic reduction of  $NO_x$  using atmospheric pressure nonthermal plasma activation of a  $Ag/Al_2O_3$  catalyst. *ACS Catalysis*, 2014, 4(2): 666–673
- Han L, Cai S, Gao M, et al. Selective catalytic reduction of  $NO_x$  with  $NH_3$  by using novel catalysts: state of the art and future prospects. *Chemical Reviews*, 2019, 119(19): 10916–10976
- Liu Z, Li J, Woo S I. Recent advances in the selective catalytic reduction of  $NO_x$  by hydrogen in the presence of oxygen. *Energy & Environmental Science*, 2012, 5(10): 8799
- Twigg M V. Progress and future challenges in controlling automotive exhaust gas emissions. *Applied Catalysis B: Environmental*, 2007, 70(1–4): 2–15
- Jung Y, Shin Y J, Pyo Y D, et al.  $NO_x$  and  $N_2O$  emissions over a Urea-SCR system containing both  $V_2O_5$ - $WO_3/TiO_2$  and Cu-zeolite catalysts in a diesel engine. *Chemical Engineering Journal*, 2017, 326: 853–862
- Xu H T, Luo Z Q, Wang N, et al. Experimental study of the selective catalytic reduction after-treatment for the exhaust emission of a diesel engine. *Applied Thermal Engineering*, 2019, 147: 198–204
- Mehregan M, Moghiman M. Experimental investigation of the distinct effects of nanoparticles addition and urea-SCR after-treatment system on  $NO_x$  emissions in a blended-biodiesel fueled internal combustion engine. *Fuel*, 2020, 262: 116609
- Koebel M, Elsener M, Madia G. Reaction pathways in the selective catalytic reduction process with  $NO$  and  $NO_2$  at low temperatures. *Industrial & Engineering Chemistry Research*, 2001, 40(1): 52–59
- Roppertz A, Fügler S, Kureti S. Investigation of urea-SCR at low temperatures. *Topics in Catalysis*, 2017, 60(3–5): 199–203
- Chen Y, Huang H, Li Z, et al. Study of reducing deposits formation

- in the urea-SCR system: mechanism of urea decomposition and assessment of influential parameters. *Chemical Engineering Research & Design*, 2020, 164: 311–323
17. Liao Y, Dimopoulos Eggenschwiler P, Rentsch D, et al. Characterization of the urea-water spray impingement in diesel selective catalytic reduction systems. *Applied Energy*, 2017, 205: 964–975
  18. Baleta J, Mikulčić H, Vujanović M, et al. Numerical simulation of urea based selective non-catalytic reduction de-NO<sub>x</sub> process for industrial applications. *Energy Conversion and Management*, 2016, 125: 59–69
  19. Liu C, Aika K I. Modification of active carbon and zeolite as ammonia separation materials for a new de-NO<sub>x</sub> process with ammonia on-site synthesis. *Research on Chemical Intermediates*, 2002, 28(5): 409–417
  20. Sandoval Rangel L, Rivera de la Rosa J, Lucio Ortiz C J, et al. Pyrolysis of urea and guanidinium salts to be used as ammonia precursors for selective catalytic reduction of NO<sub>x</sub>. *Journal of Analytical and Applied Pyrolysis*, 2015, 113: 564–574
  21. de Mattos Lourenço Á A, Martins C A, Lacava P T, et al. Selective catalytic reduction study with alternative reducing agents. *Environmental Engineering Science*, 2013, 30(5): 221–231
  22. Fulks G, Fisher G B, Rahmoeller K, et al. A review of solid materials as alternative ammonia sources for lean NO<sub>x</sub> reduction with SCR. *SAE Technical Paper Series*, Warrendale, PA, USA, 2009
  23. Johannessen T, Schmidt H, Svagin J, et al. Ammonia storage and delivery systems for automotive NO<sub>x</sub> after treatment. *SAE Technical Paper Series*, Warrendale, PA, USA, 2008
  24. Elmøe T D, Sørensen R Z, Quaade U, et al. A high-density ammonia storage/delivery system based on Mg(NH<sub>3</sub>)<sub>6</sub>Cl<sub>2</sub> for SCR-DeNO<sub>x</sub> in vehicles. *Chemical Engineering Science*, 2006, 61(8): 2618–2625
  25. Lysgaard S, Ammitzbøll A L, Johnsen R E, et al. Resolving the stability and structure of strontium chloride amines from equilibrium pressures, XRD and DFT. *International Journal of Hydrogen Energy*, 2012, 37(24): 18927–18936
  26. Jiang L, Xie X L, Wang L W, et al. Performance analysis on a novel self-adaptive sorption system to reduce nitrogen oxides emission of diesel engine. *Applied Thermal Engineering*, 2017, 127: 1077–1085
  27. Jiang L, Xie X L, Wang L W, et al. Investigation on an innovative sorption system to reduce nitrogen oxides of diesel engine by using carbon nanoparticle. *Applied Thermal Engineering*, 2018, 134: 29–38
  28. Wang Z X, Wang L W, Gao P, et al. Analysis of composite sorbents for ammonia storage to eliminate NO<sub>x</sub> emission at low temperatures. *Applied Thermal Engineering*, 2018, 128: 1382–1390
  29. Gao P, Wang L W, Wang R Z, et al. Optimization and performance experiments of a MnCl<sub>2</sub>/CaCl<sub>2</sub>-NH<sub>3</sub> two-stage solid sorption freezing system for a refrigerated truck. *International Journal of Refrigeration*, 2016, 71: 94–107
  30. Wu S, Li T X, Yan T, et al. Experimental investigation on a novel solid-gas thermochemical sorption heat transformer for energy upgrade with a large temperature lift. *Energy Conversion and Management*, 2017, 148: 330–338
  31. An G L, Wang L W, Gao J. Two-stage cascading desorption cycle for sorption thermal energy storage. *Energy*, 2019, 174: 1091–1099
  32. Kang Y, Wei S, Zhang P, et al. Detailed multi-dimensional study on NO<sub>x</sub> formation and destruction mechanisms in dimethyl ether/air diffusion flame under the moderate or intense low-oxygen dilution (MILD) condition. *Energy*, 2017, 119: 1195–1211
  33. Wang L, Wang R, Wu J, et al. Research on the chemical adsorption precursor state of CaCl<sub>2</sub>-NH<sub>3</sub> for adsorption refrigeration. *Science in China Series E: Technological Sciences*, 2005, 48(1): 70–82
  34. Jiang L, Wang L W, Wang R Z. Investigation on thermal conductive consolidated composite CaCl<sub>2</sub> for adsorption refrigeration. *International Journal of Thermal Sciences*, 2014, 81: 68–75
  35. Xu Q, Fang Z, Chen Y, et al. Titania-samarium-manganese composite oxide for the low-temperature selective catalytic reduction of NO with NH<sub>3</sub>. *Environmental Science & Technology*, 2020, 54(4): 2530–2538
  36. Han M, Jiao Y, Zhou C, et al. Catalytic activity of Cu-SSZ-13 prepared with different methods for NH<sub>3</sub>-SCR reaction. *Rare Metals*, 2019, 38(3): 210–220
  37. Meng B, Zhao Z, Chen Y, et al. Low-temperature synthesis of Mn-based mixed metal oxides with novel fluffy structures as efficient catalysts for selective reduction of nitrogen oxides by ammonia. *Chemical Communications (Cambridge)*, 2014, 50(82): 12396–12399